韓放技學誌, Vol.14, No.2, 1991

SPECT 영상에서 불균등 감약물질의 콤프톤 산란 분포함수

원광보건전문대학 방사선과
이 만 구

Abstract

Compton Scatter Distribution Function in Non-uniform Attenuation Media in SPECT

Man Koo Lee

Dept. of Radiotechnology, Wonkwang Public Health Junior College

SPECT 영상에서 콤프톤 산란 광자는 공간분해능의 감소와 그 양을 측정하는데 있어 정확성과 정밀성을 감소시킨다. 이와같은 콤프톤 산란의 영향을 감소시키기 위하여 사용하는 대부분의 보정방법은 선원의 위치로부터 거리의 단일지수함수로 대칭인 산란분포함수를 고려하게 된다. 본 연구는 균등 및 불균등 산란에 대한 산란분포함수를 얻기 위하여 보다 현실적인 접근방법을 시도하였다.

산란 및 비산란광자의 공간분포와 에너지분포를 얻기 위하여 뼈, 폐, 물의 균등 및 불균등 분포로 된 원통형의 팬톰 속에 ^{99m}Tc의 선선원 및 점선원을 놓고 Monte Carlo Simulation을 하였으며, 깊이의 함수, media의 접촉영역으로부터 선원거리 및 산란체의 밀도의 변화로 표현한 산란분포함수(SDF)를 얻었다. 산란분포함수는 균등한 뼈, 폐, 물에서는 선원위치로부터 거리의 단일지수함수(single exponential functions)로 대칭으로 나타났으며, 두 물체의 조합에서는 2중지수함수(dual exponential functions)로 비대칭으로 나타났다. 산란분율은 20% window photopeak에서 총 계수의 8%에서 53%까지 다양한 변화가 있었으며, 지수함수의 기울기는 0.1~0.9 cm^{-1}의 범위로 나타났다. 불균등 산란체에서 얻은 산란분포함수는 SPECT 영상에 있어 콤프톤 산란의 감소에 대한 보다 정확한 보정방법의 개발에 필요한 정보를 제공할 것이다.

I. Introduction

For single photon emission computed tomography (SPECT) to become more widely used, it will be necessary to provide accurate quantitation of active levels. SPECT images are both qualtatively and quantitatively degrade by attenuation, scattering, camera non-uniformity and limited spatial resolution effects. Compton scattered photons degrade spatial resolution and reduce the accuracy and precision of quantitation in SPECT images, to improve the accuracy of the SPECT measurement, compensation methods need to be used. AS noted by Oppenheim[1], the problem for Compton scatter has received less attention than attenuation and camera non-uniformity, perhaps becau-

se the latter problems can produce dramatic effects on the reconstructed image. Consideration of scatter is important since its inclusion in the SPECT data set degrades the contrasts of lesions and results in a major source of error in the quantification of radionuclide concentrations. The majority of correction methods introduced to reduce influence of Compton scatter component consider the scatter distribution function to be a symmetrical, monoexponential function of distance from source position. The effects of attenuation and scatter have been studied by many investigators[2~8], but most have not emphasised source geometry, by which I mean both non-uniform attenuation and the radioactivity distribution itself.

Here a more realistic approach has been taken to derive scatter distribution functions for uniform and non-uniform scattering geometries.

II. Materials and methods

Monte Carlo simulations of ^{99m}Tc point and line sources were used to obtain detailed information on the spatial and energy distribution of scattered and non-scattered events in SPECT images. EGS4 simulation code was adapted for use with planar and SPECT imaging geometries and detection devices. Simulations were carried out in two steps : 1) Photons were followed in attenuation media until they were completely absorbed or emerged. Photon energy, input and output coordinates, direction and scatter order were recorded for photons that emerged within the detector field of view. 2) The detection process was simulated in a second step which gave greater flexibility in changing detection parameters(collimator geometry, intrinsic spatial resolution, energy resolution, energy window settings, etc.). Scatter in the collimator and septal penetration were not included. Energy resolution of the system was simulated by sampling from an energy-dependent Gaussian function.

The data shown were obtained from a simulation of a SPECT system with a LEHR collimator, radius of rotation of 13 cm, an energy resolution of 13%, intrinsic spatial resolution of 3.6 mm, an energy window of 20% centered at 140 keV and a pixel size of 1 mm. Separate images were obtained for nonscattered events and events of scatter order $n=1-3$; a single image was obtained for $n \geqq 4$.

1. Source and media geometry simulation

A source 1 mm in diameter and 1 mm~10 cm long was placed in a cylindrical phantom with a) uniform and b) nonuniform distributions of water, lung and bone media. The central axis of the phantom was parallel to the collimator plane.

a) Uniform geometry : source placed on-and off-axis of rotation in cylinders with radii of 6 cm and 11 cm by 21 cm long.

b) Nonuniform geometry :

1) "Stack" cylinders geometry with cylinder diameter D=12 cm and 21 cm long(L_1+L_2) (Fig. 1). Point source was placed at 0.5, 1.0, 1.5, 2.0 and 3.0 cm from media interface(D_b) at each side of the interface. Three boundary combinations were evaluated : bone/lung, water/lung and bone-

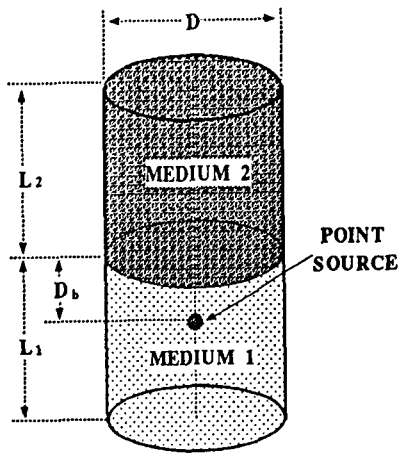

Fig. 1. "Stack" cylinder geometry

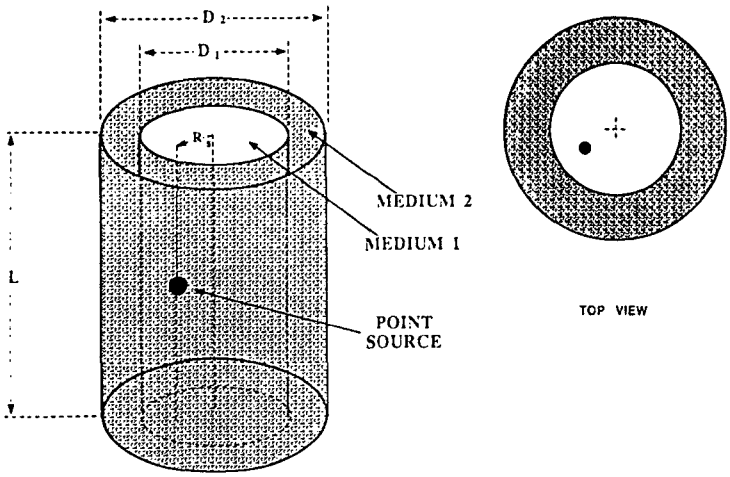

Fig. 2. Concentric cylinder geometry

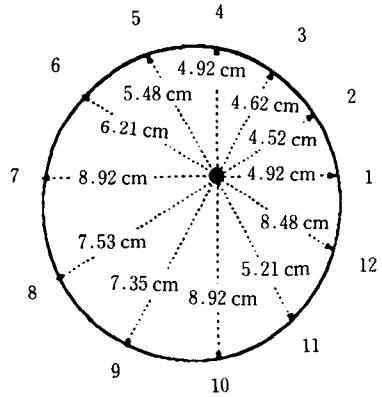

Fig. 3. Off−axis source geometry in uniform media

/water. 2) Concentric cylinders geometry (Fig. 2, 3) with inner cylinder diameter $D_1 = 12$ cm and outer cylinder diameter $D_2 = 22$ cm and length $L = 21$ cm. Source is placed in inner cylinder on−axis ($R_s = 0$ cm) and off−axis ($R_s = 3$ cm) of rotation.

2. Evaluation of Compton scatter component

Scatter fractions SFP (ratio of scatter to non−scatter counts) and SFT (ratio scatter to total counts) were evaluated as function of media density and depth from phantom surface. The scatter distribution function (SDF) as a function of distance from the source position was obtained for each set of simulated projection data. SDFs were evaluated as a function of depth, density of the media and source distance from the two media interface. SDF for uniform medium was fitted to a single exponential function and SDF in nonuniform media was fitted to a dual exponential function.

III. Results

Scatter fractions calculated for off−axis source geometry as function of depth in the medium. Scatter fractions vary from 8% to 54% of total counts observed in 20% window over the photopeak and the slope of experimental functions display a range of 0.1 to 0.9 cm^{-1} (Table 1, Fig. 1).

Scatter distribution functions were symmetrical monoexponential functions of distance from source position. Slope of exponential function does not depend on scattering media, but strongly depends on cylinder radius (Table 2).

Scatter distribution functions in non−uniform media were clearly asymmetrical dual exponential functions at bone/lung and water/lung boundaries, SDF for lung/bone and lung/water boundary show a secondary peak in close proximity to the boundary.

Table 1. Calculated scatter fractions for source in center of uniform cylinder

	Radius=6 cm		Radius=11 cm	
Medium	SFT	SFP	SFT	SFP
Lung	0.08	0.09	0.14	0.16
Water	0.26	0.35	0.66	0.40
Bone	0.39	0.64	0.54	1.20

Table 2. Amplitudes and slopes for SDFs

	Radius=6 cm		Radius=11 cm	
Medium	Amplitude (arb. units)	Slope (mm^{-1})	Amplitude (arb. units)	Slope (mm^{-1})
Lung	0.0032	0.070	0.0031	0.040
Water	0.0094	0.071	0.0084	0.041
Bone	0.0142	0.073	0.0119	0.043

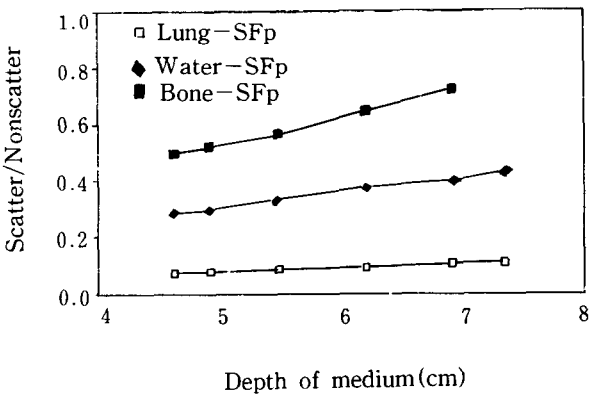

Fig. 4. Scatter fractions calculated for off−axis source geometry as function of depth in medium

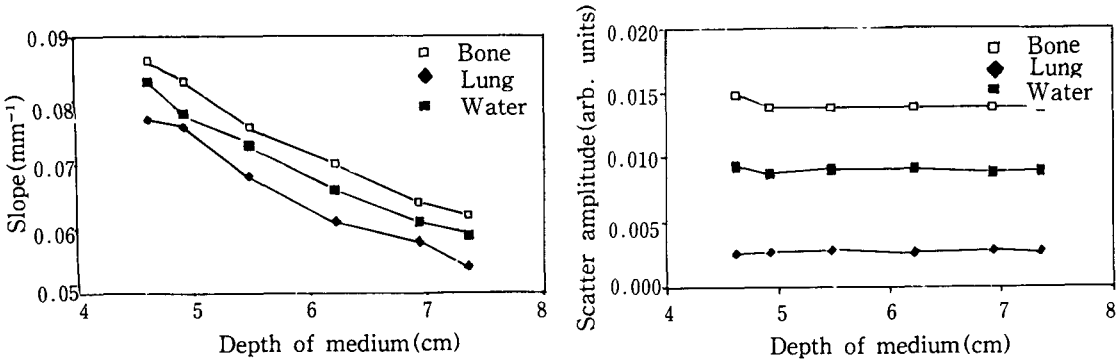

Fig. 5. Amplitudes and slopes for off−axis SDFs

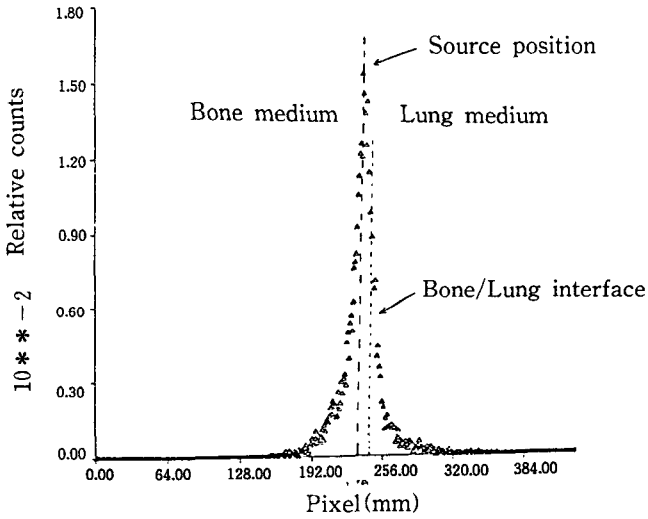

Fig. 6. Scatter distribution function for point source in bone medium, positioned 1 cm from bone/lung interface

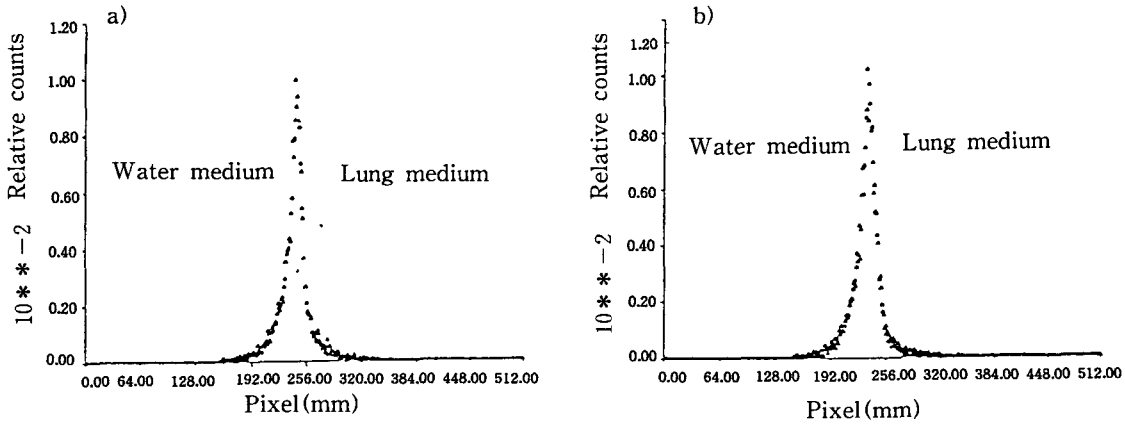

Fig. 7. SDF's for source in water at a) 0.5 cm and b) 1.5 cm from water/lung boundary

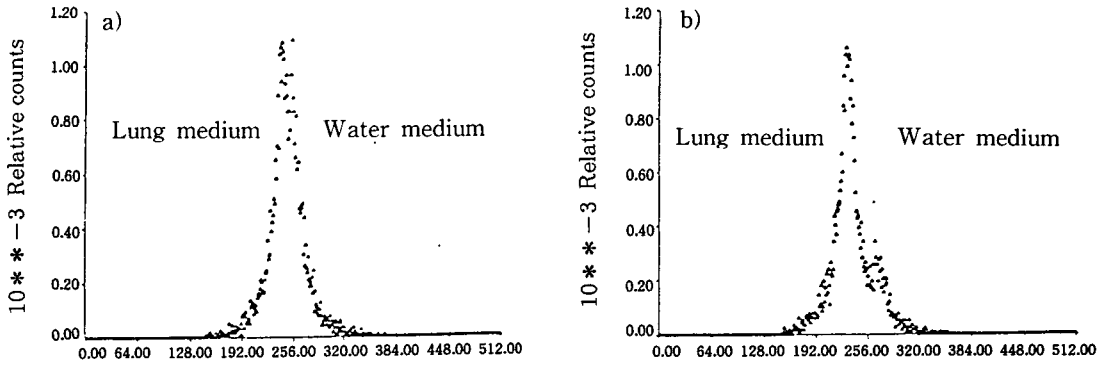

Fig. 8. SDF's for source in lung at a) 1.0 cm and b) 3.0 cm from lung/water boundary
Relative counts Pixel(mm) Water medium Lung medium a) b) 10 * * −3

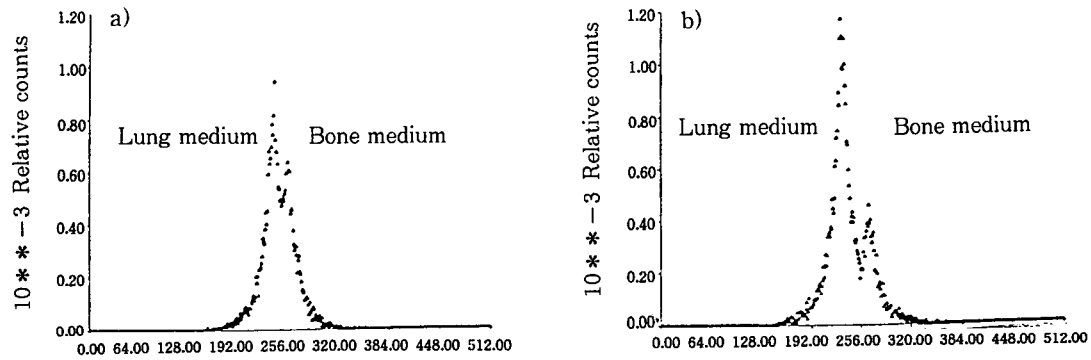

Fig. 9. SDF's for source in lung at a) 1.5 cm and b) 3.0 cm from lung/bone boundary

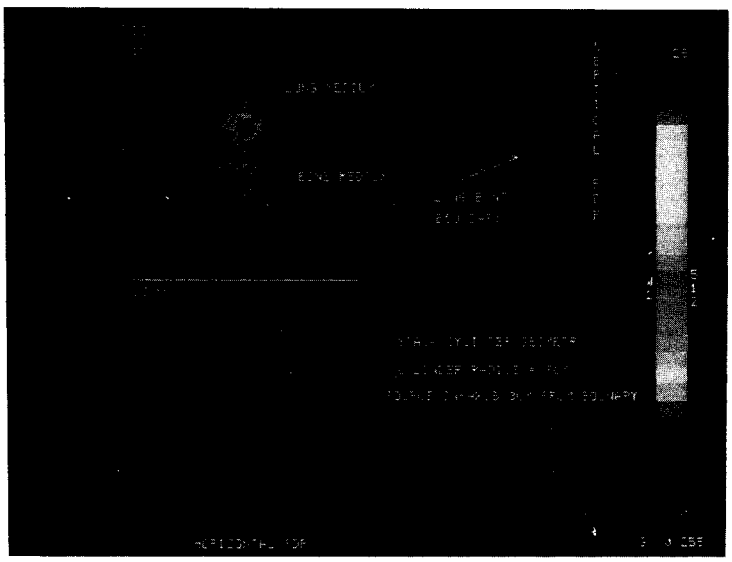

Fig. 10. Spatial distribution of scattered photons and SDFs for source in lung media placed on−axis of cylinder(R=6 cm), at distance of 3 cm bone boundary

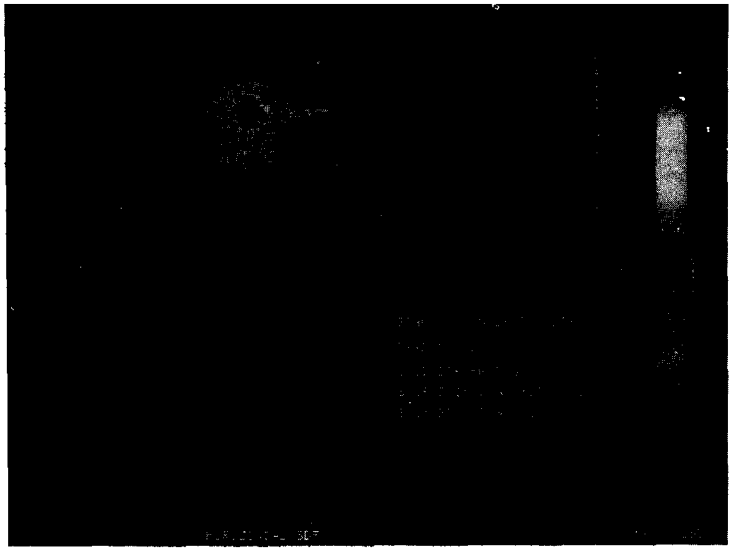

Fig. 11. Reconstructed sagittal projection and SDFs for scatter distribution of the source in lung media 3 cm from bone boundary. Data were reconstructed using filtered back projection with Shepp−Logan filter.

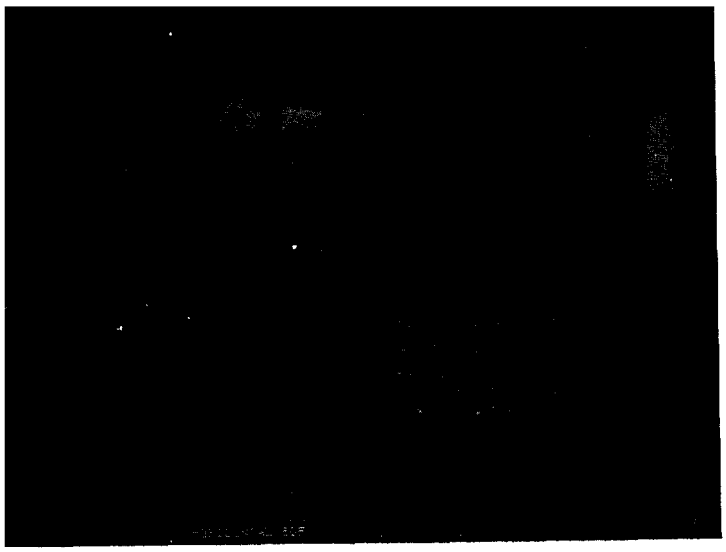

Fig. 12. Reconstructed sagittal projection and SDFs for scatter distribution of the source in lung media 3 cm from water boundary. Data were reconstructed using filtered back projection with Shepp−Logan filter.

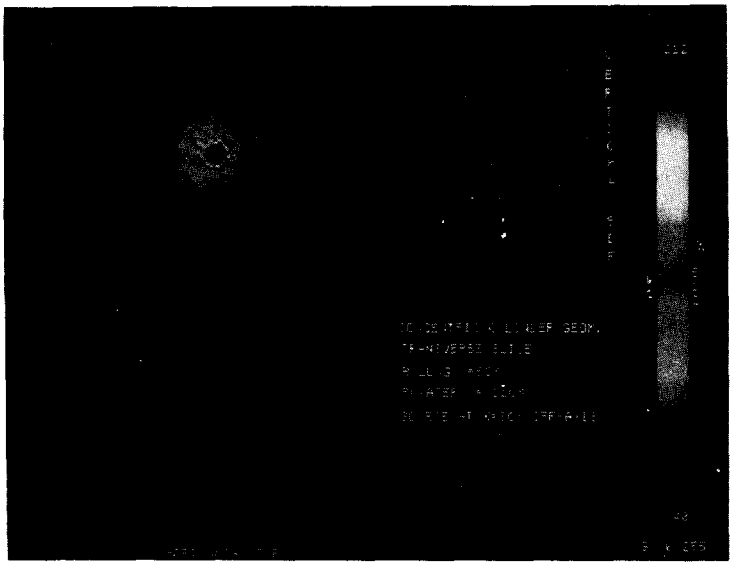

Fig. 13. Reconstructed transverse projection and SDFs for scatter distribution of the source in lung media off-axis at y=3 cm in concentric geometry with R(lung)=6 cm and R (water)=11 cm. Data were reconstructed using filtered back projection with Shepp-Logan filter.

IV. Conclusion

The scatter distribution function in non-uniform density media indicates that scatter correction techniques based on single exponential scatter distribution function do not provide a valid correction for nonuniform scattering geometries. Further investigations of SDF in more complex non-uniform geometries are needed to develop accurate correction method for Compton scatter reduction in SPECT images. My results suggest that 3-D scatter correction function and reconstruction methods need to be applied.

References

1. Oppenheim B.E. : Scatter correction for SPECT, J. Nucl. Med. 25 928~929, 1984.
2. Takao Mukai, Jonathan M. Links, Kenneth H. Douglass and Henry N. Wagner Jr : Scatter correction in SPECT using non-uniform attenuation data, Phys. Med. Biol. 33 1129~1140, 1988.
3. Censor Y, Gustafson D.E., Lent A. and Tuy H. : A new approach to the emission computerized tomography problem : Simultaneous calculation of attenuation correction and activity coefficients, IEEE Trans. Nucl. Sci. NS-26 2775~2779, 1979.
4. Egbert S.D. and May R.S. : An integral-transport method for Compton-scatter correction in emission computed tomography, IEEE Trans. Nucl. Sci. NS-27 543~548, 1980.
5. Beck J.W., Jaszczak R.J., Coleman R.E., Starmer C.F. and Nolte L.W. : Analysis of SPECT including scatter and attenuation using sophisticated Monte Carlo modeling method, IEEE Trans. Nucl. Sci. NS-29 506~511, 1982.
6. Jaszczak R.J., Greer K.L., Floyd C.E., Harris C.C. and Coleman R.E. : Improved SPECT quantitation using compensation for scattered photon, J. Nucl. Med. 25 893~900, 1984.

7. Axelsson B., Msaki P. and Israelsson A. : Subtraction of Compton scattered photon emission computed tomography, J. Nucl. Med. 25 490～494, 1984.

8. Floyd C.E., Jaszczak R.J., Greer K.L. and Coleman R.E. : Deconvolution of Compton scatter in SPECT, J. Nucl. Med. 26 403～408, 1985.